BEAM TEST RESULTS OF THE INS RFQ/IH LINAC

S. Arai, Y. Arakaki, Y. Hashimoto, A. Imanishi, T. Katayama, H. Masuda, K. Niki, M. Okada,
Y. Takeda, E. Tojyo, N. Tokuda[†], M. Tomizawa, K. Yoshida, and M. Yoshizawa
Institute for Nuclear Study, University of Tokyo
3-2-1 Midori-cho, Tanashi, Tokyo 188, Japan
[†] KEK, National Laboratory for High Energy Physics
1-1 Oho, Tsukuba, 305 Japan

Abstract

A linac complex for radioactive beams has been constructed at INS, which comprises a 25.5-MHz split coaxial RFQ (SCRFQ) with modulated vanes and a 51-MHz interdigital-H (IH) linac . The SCRFQ accelerates ions with a charge-to-mass ratio (q/A) greater than 1/30 from 2 to 172 keV/u. The beam from the SCRFQ is charge-stripped by a carbon-foil, and is transported to the IH linac through two magnetic-quadrupole doublets and a 25.5-MHz rebuncher cavity. The IH linac accelerates ions with a q/A greater than 1/10, and the output energy is variable in the range of 0.17 through 1.05 MeV/u. Beam tests of the linac complex performed with N^{2+} ions show that the output beam energy and transmission efficiency agree well with predictions.

Introduction

A short-lived nuclear beam acceleration facility has been constructed at INS, which is a prototype for the exotic nuclei arena of the Japanese Hadron Project [1]. The facility comprises an SF cyclotron, an ISOL and a heavy-ion linac complex. The short-lived nuclei, produced by bombarding a thick target with a 40-MeV 10-μA proton beam from the existing SF cyclotron, are ionized in an ion source, mass-analyzed by the ISOL, and transported to the linac complex through a 60-m long beam line. The linac complex comprises a 25.5-MHz split coaxial RFQ (SCRFQ) with modulated vanes and a 51-MHz interdigital-H (IH) linac, as shown in Fig. 1.

As a front-end structure of the linac complex, we employed an SCRFQ, because the cavity diameter is smaller than 1 m even at a low frequency such as 25.5 MHz. The SCRFQ accelerates ions with a q/A greater than 1/30 from 2 to 172 keV/u [2]. After charge stripping, the IH linac, 5.63 m in total length, accelerates ions with a $q/A \geq 1/10$ up to 1.05 MeV/u, which comprises four tanks and three magnetic-quadrupole triplets between tanks [3]. Since the tanks are excited separately by four rf sources, it is possible to vary the output beam energy continuously in a range from 0.17 to 1.05 MeV/u by adjusting the rf power levels and phases. The duty factor of the linac complex depends on q/A of the ions: nearly 100% at $q/A \geq 1/16$, and given by $270 \times (q/A)^2 \times 100\%$ at $1/17 \geq q/A \geq 1/30$.

In the stage of completion of the SCRFQ, the low-energy beam transport (LEBT), and first quadrupole doublet in the medium-energy beam transport (MEBT), we conducted beam tests of the SCRFQ, by using stable-nucleus ions, N^+. After beam tests, the IH linac, the rebuncher cavity, the second quadrupole doublet in the MEBT, and a momentum analyzer in a high-energy beam transport (HEBT) were aligned precisely on the beam line down the SCRFQ. After low-power tests of the IH and rebuncher cavities, we conducted their high-power tests for aging the cavities. On March 29, 1996, we succeeded in the first acceleration of the SCRFQ/IH linac with a N^{2+} beam. This paper describes the linac construction and the beam test results.
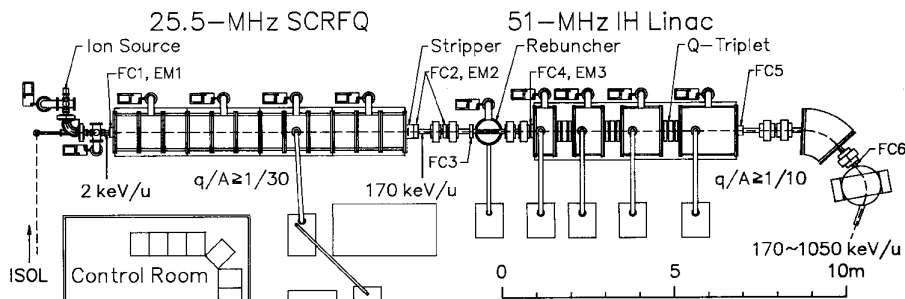

Figure 1: Layout of the heavy-ion linac system.

Split Coaxial RFQ (SCRFQ)

Construction of the cavity

The SCRFQ has been constructed on the basis of the studies of a prototype. Design parameters of the SCRFQ are summarized in Table 1. The cavity (0.9 m in inner diam., 8.6 m in length) comprises four unit cavities, whose structure is nearly same as that of the prototype. In the new cavity, we didn't use the vane coupling rings installed in the prototype, because they caused appreciable shift of the resonant frequency in high-power operations. The unit cavity comprises three module-cavities as shown in Fig. 2. The material of the tank is mild steel, whose inner wall is plated with copper to a thickness of 100 μm, and that of the inner structure except the vanes and spacing rods is oxygen-free copper. The vanes are made of chromium-copper alloy containing Cr of 1%, and the spacing rods are copper plated stainless steel.

Table 1
Design parameters of the 170 keV/u SCRFQ

Frequency (f)	25.5 MHz
Charge-to-mass ratio (q/A)	$\geq 1/30$
Kinetic energy (T)	$2 \rightarrow 172$ keV/u
Input emittance (ε_{in})	29.1 π cm·mrad
Normalized emittance (ε_n)	0.6π mm·mrad
Vane length (l_V)	8.585 m
Number of cells (radial matcher)	172 (20)
Intervane voltage (V)	108.6 kV
Max. surface field ($E_{s,max}$)	178.2 kV/cm
	(2.49 Kilpatrick)
Mean aperture radius (r_0)	0.9846 cm
Minimum aperture radius (a_{min})	0.5388 cm
Max. modulation index (m_{max})	2.53
Margin of bore radius (a_{min}/a_{beam})	1.2
Final synchronous phase (ϕ_f)	$-30°$
Focusing strength (B)	5.5
Max. defocusing strength (Δ_b)	-0.17
Transmission efficiency*	
at 0 mA input	91.4%
at 5 mA input	86.0%

*(for q/A=1/30 ions)

The module length, 0.7 m, was determined so as that the droop of the vanes due to the gravity might not exceed 35 μm, and the cavity diameter, 0.9 m, so as that the resonant frequency might be 25.5 MHz. The electrodes comprising the vanes and the spear-shaped back plates are supported by stems. The stem-flanges are arranged at equal distances by spacing-rods. By introducing the spacing-rods, it became possible to align the vanes with an accuracy better than ± 40 μm before installation in the unit-cavity tank. The unit cavity is cooled by eleven water channels running in parallel. Total flow rate for one unit cavity is about 290 l/min, and the temperature increase of the water is less than 1.4°C under a 30% duty operation with a peak power of 90 kW. After completion of the four unit-cavities, we aligned them in an accelerator room with an error less than ± 50 μm.

The vane tip geometry has following features: the transverse radius of curvature of the vane-tip (ρ_T) is variable in the low-energy part, about 1 m long in the first unit cavity, and the ρ_T is constant at the mean aperture radius (r_0) in the high-energy part. The vanes in the first unit cavity were machined by means of a three-dimensional cutting technique, and for the other vanes a two-dimensional cutting technique was used. For each vane-tip geometry, we made a correction on the aperture parameter a and modulation m (A_{10} correction) to bring the actual field close to an ideal one.
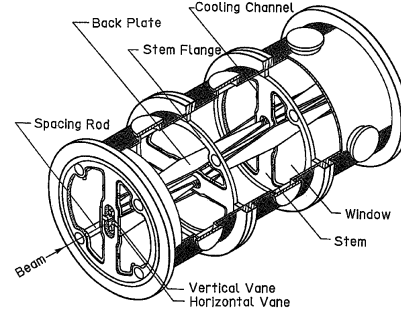

Figure 2: Structure of the unit cavity.

Rf aspects

We tuned the resonant frequency and the longitudinal voltage distribution by changing locally the inter-electrode capacitance and the stem inductance. For changing the capacitance, C-tuners of the copper plates (170 or 120 mm in height, 30 mm in width, 3 mm in thickness) were attached on the back-plates so that a plate confronted a stem with a distance of 25 mm. In order to flatten the longitudinal voltage distribution, C-tuners (170 mm in height) were installed in the 1st module, and other tuners (120 mm in height) in the 2nd and 12th ones; the number of tuners is four per module. Further fine tuning was performed by adjusting the stem inductance between the 6th and 7th modules. After tuning, the longitudinal distribution was flat within $\pm 1\%$, and the azimuthal field imbalance within $\pm 1\%$. The resonant frequency was 25.46 MHz, and the unloaded Q-value 5800. From their values and total capacitance between electrodes, 1616 pF, the resonant resistance (R_p) is derived to be 22 kΩ. The final tuning to 25.5 MHz is performed by means of piston tuners.

The high-power operation was conducted for aging the cavity and for calibration of the intervane voltage (V_{vv}). The rf source generates a max. power of 350 kW in peak with a duty factor of 30%. The input power (P_{in}) is transmitted into the cavity through a 6-m coax (WX-120D) and a loop coupler. By using four 500-l/s turbo-molecular pumps, the cavity is kept at a vacuum of 5×10^{-7} Torr without power input. So far, we have achieved the goal intervane voltage of 109 kV at a duty factor of 15%.

We figure out intervane voltage from the output voltage (V_{ML}) of a monitor loop attached to the 12th module cavity. We obtained the calibration constant, $V_{vv}/V_{ML} = 10,388$, by measur-

ing the endpoint energy of X-ray from cavity. From the relation, $R_\mathrm{p} = V_\mathrm{vv}^2/2P_\mathrm{in}$, the resonant resistance was derived to be 24.55 $\pm\,0.44$ kΩ under high-power operation. This value is higher than 22 kΩ, which we obtained in low-power test. The increase of the resonant resistance may be due to the Q-value improvement through the aging.

Interdigital-H Linac

Construction of the cavities

The design parameters of the IH linac are listed in Table 2 together with the low-power test results. The synchronous phase is $-25°$ to assure a stable longitudinal motion. In order to obtain the high shunt impedance, the accelerating mode is π-π, and no transverse focusing element is installed in the drift tubes. The inner diameters of the 1st through 3rd tanks are a little bit larger than that of 4th one, so that the resonant frequencies are kept to 51 MHz without reducing the shunt impedance. Each gap length between drift-tubes is equal to one half of the first cell length. Both end structures of the cavity, *i.e.*, the magnetic flux inducers and the gaps between end-wall and ridge, are determined experimentally so as that the longitudinal field distribution becomes flat over a cavity.

The material of the tank is mild steel, whose inner wall is plated with copper to a thickness of 100 μm, and that of the ridges, drift-tubes and stems is oxygen-free copper. For tuning the cavity, three kinds of tuners are used: a capacitive tuner (C-tuner), four inductive end tuners (end L-tuner), and an inductive piston tuner (L-tuner). The C-tuner is a manually movable disk (19 cm in diam.) facing a ridge. The L-tuner is moved automatically to compensate the frequency shift due to the temperature change. The structure of the 4th tank is illustrated in Fig. 3.
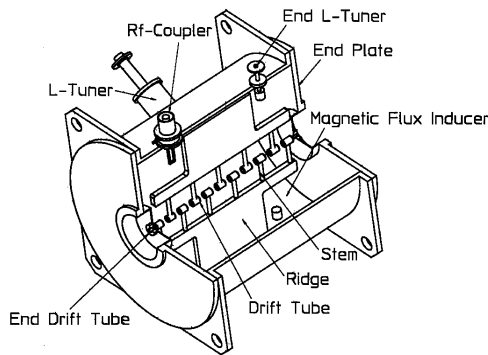

Figure 3: Structure of the IH-linac tank4.

Rf aspects

The results of the low-power tests are summarized in Table 2. The resonant frequencies (f_initial) of four tanks were tuned with C-tuners to 51 MHz (f_tuned). Without any particular tuning, we obtained the gap-voltage distributions almost flat except at the tank ends. From the measured unloaded Q-values (Q_o) and

field distributions in the gaps, we figured out effective shunt impedances (Z_eff), and then the rf powers (P) required for accelerating the $q/A = 1/10$ ions up to 1.05 MeV/u.

Table 2
Design parameters and low-power test results of the IH linac

	Tank1	Tank2	Tank3	Tank4
T_out (keV/u)	294	475	725	1053
L_tank (cm)	68	90	115	153
D_tank (cm)	149	149	149	134
R_bore (cm)	1.0	1.2	1.4	1.6
$D_\mathrm{d.tube}$ (cm)	3.8	4.4	4.6	5.2
No. of cells	9	10	11	12
V_gap (kV)	200	250	315	370
f_initial (MHz)	51.084	51.134	51.180	51.003
f_tuned (MHz)	51.000	51.000	51.000	51.000
Q_o	10681	15387	16230	18490
Z_eff (MΩ/m)	264	289	268	218
P (kW)	10.5	15	25	39
ΔV_gap (%)	±2.0	±2.9	±3.5	±2.2

The capacities of the rf sources for the 1st through 4th tanks are 12kW, 22kW, 30kW and 50kW, respectively. The rf sources were connected to the tanks through about 20-m coaxes (WX-77D for the 1st through 3rd tanks, WX-120D for the 4th tank). Each of the 1st and 2nd tanks is evacuated by a 500-l/s turbo-molecular pump, and each of the 3rd and 4th tanks is by a 1500-l/s one. The obtained vacuum pressures are in the range of 10^{-7} Torr under no power feed. The high-power aging was conducted for the N^{2+} beam acceleration test, in which 70% of the max. gap voltage was required at a duty factor of 15%. The time spent in aging conducted at a duty factor of about 20% was about 12 hours per cavity.

Beam Transports

As shown in Fig. 1, the LEBT consists of a 2.45-GHz ECR ion source, a 90° bending magnet, two quadrupole magnets, and four einzel lenses [4]. The ion source produces stable nucleus beams. The bending magnet separates ions with different charge-to-mass ratios. The quadrupole magnets are used for making the vertical beam size small in the bending magnet and for matching the transverse phase spaces at two focal points. The momentum resolution of the ion separating system is 0.65%. A double-slit emittance monitor (EM1) and a Faraday cup (FC1) are installed at the RFQ entrance.

The MEBT between the SCRFQ and the IH linac comprises a charge stripper (carbon foil of 10 μg/cm^2), a rebuncher and two quadrupole doublets [4]. This transport system has a total length of 3.76 m. Since the frequency of 25.5 MHz was required for the rebuncher, a double-coaxial resonator with 6 gaps was developed to maintain the size small and power low [5]. The emittance monitor (EM2) is separated into two parts: the front slit is near the RFQ exit, and the rear one is between the quadrupole magnets. The Faraday cup FC2 measures the current of drift-

through ions (both of accelerated and unaccelerated ions), and FC3 the current of accelerated ions only. The emittance monitor (EM3) and the Faraday cup (FC4) were located at the entrance of the IH linac. The EM3 comprises four moving slits. The vacuum chamber containing EM3 and FC4 was made compactly so as to be installed in a small space (38 cm in diam. and 15 cm in length) just before the first tank of the IH linac. The Faraday cup (FC5) cooled by a water channel was located at the exit of the IH linac. The momentum analyzing system in the HEBT was set up at the downstream of the IH linac. This comprises a quadrupole doublet, a dipole magnet, a vertical slit with a width of 4 mm and a charge collecting plate (FC6). This system has a energy resolution of less than 1% for the 1-MeV/u ion beam, which has the design emittance of the IH linac. The beam energy was estimated from the magnetic field measured by a hole probe.

Beam Tests

Performance of the SCRFQ

We measured the transmission efficiency as a function of the intervane voltage. The RFQ operated at 25.47 MHz with a duty factor of 5%. The N^+ beam had the input emittances, 17 and 22 π cm·mrad in the x-x' and y-y' planes, and the current was about 0.22 mA in peak at FC1. The measurement result is shown in Fig. 4 along with a simulation. The horizontal scale is the normalized intervane voltage, $V_n = V_{vv}/50.68$ kV. The measured transmission efficiency of drift-through ions (◦ in the figure) is defined by $I(FC2)/I(FC1)$, where $I(FCi)$ is the beam current from the Faraday cup i, and that of accelerated ions (●) by $I(FC3)/I(FC1)$. The simulation was done by using the PARMTEQ-H version including the higher-order-multipole fields calculated by Crandall [6]. At the nominal intervane voltage ($V_n = 1$) the measured transmission efficiency is 90%. This is close to the designed value of 91.4% with a matched input beam with $\varepsilon_n = 0.06$ π cm·mrad. The measured output emittance profiles were inside of the design ellipses, with $\varepsilon_n = 0.06$ π cm·mrad.
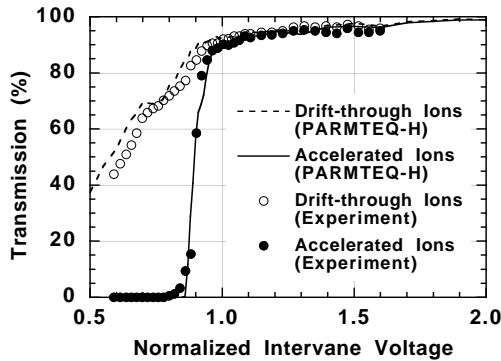

Figure 4: Transmission efficiencies vs normalized intervane voltage.

Performance of the linac complex

The overall performance of the SCRFQ/IH linac was examined by using a N^{2+} beam. The beam intensity at the entrance of the SCRFQ is about 1 μA at peak in a pulse operation, 0.6 ms in width and 100 Hz in repetition rate. The rf pulse widths of the SCRFQ and IH linac were set to 1.5 ms so as to cover the beam pulse from the ion source. The 25.5 MHz-rebuncher was operated at 100% duty. The beam accelerated by the SCRFQ was directly injected to the IH linac without using the stripping foil.

Before measuring the beam performance, we adjusted the gap voltage and rf phase of each IH tank to the design values, because the output beam energy and its spread from the IH linac are very sensitive to those parameters. In Fig. 5, the output energies are plotted as a function of the rf phase of the tank4; figure (a) shows a simulation, and figure (b) a measurement. In the simulation, they were calculated at the design gap voltage.
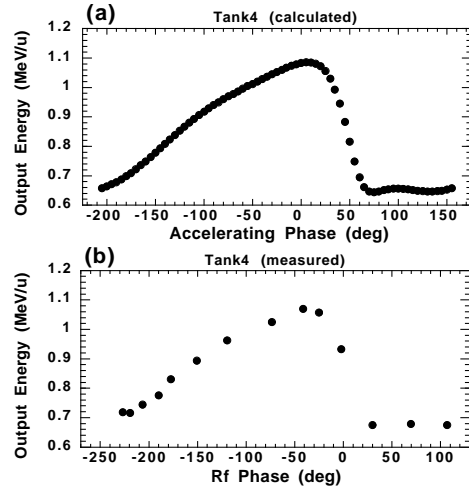

Figure 5: Output beam energy vs accelerating phase; (a) is the simulation and (b) the measurement.

If the beam with a design energy is injected into the tank4, we can adjust the gap voltage and the rf phase experimentally by comparing the measured function with the simulated one. As a result, we set the gap voltage and rf phase to give the nominal output energy. The voltages and phases of the other tanks were also set by the same method as that for tank4.

After adjusting the gap voltage and rf phase, we optimized parameters of the focusing elements to increase the transmission efficiency of the IH linac. Figure 6 shows the beam energy spectra measured at six operating modes, and figure 7 the transmission efficiencies of almost 100% for five operating modes. For example, "IH-Tank3" in the figure shows the result obtained when the SCRFQ and the 1st through 3rd IH-tanks are operated and the 4th tank is not operated.

As seen from "IH-Tank4", the beam was accelerated up to the max. design energy, 1.05 MeV/u. The measured energy spreads ($\Delta T/T$) are listed in Table 3 with the calculated values given in
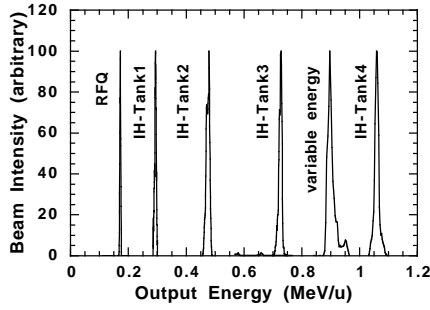
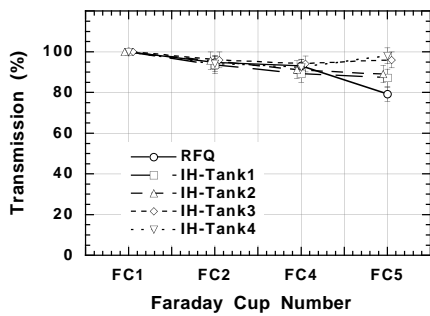Figure 6: Energy spectra for six operating modes.

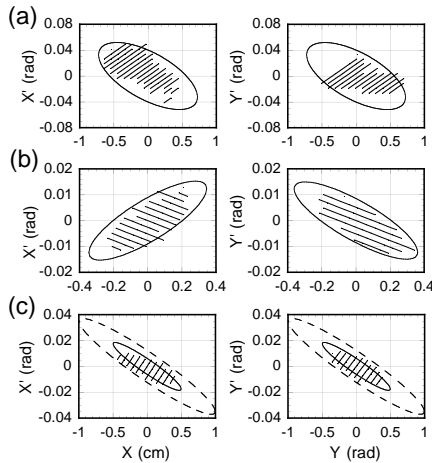Figure 7: Transmission efficiency for five operating modes.

Figure 8: (a) Emittance profiles at the RFQ entrance, (b) at the RFQ exit, and (c) at the IH-linac entrance.

parentheses, where ΔT is defined by 2σ of the spectrum containing 90% ions. The emittance profiles were measured at the RFQ entrance, the RFQ exit and the IH-linac entrance as shown in Fig. 8. The bars indicate measured 90% emittance profiles of a N^{2+} beam, and the solid-line ellipses the designed ones with

an area of $\varepsilon_n = 0.06$ π cm·mrad. The broken-line ellipses in figure (c) show the designed acceptance of the IH linac with 0.24 π cm·mrad normalized.

Table 3
Output energies and energy spreads for five operating modes

	RFQ	Tank1	Tank2	Tank3	Tank4
T (keV/u)	172	293	476	726	1059
	(172)	(294)	(475)	(725)	(1053)
$\Delta T/T$ (%)	1.56	1.65	1.97	1.15	1.12
	(1.06)	(1.77)	(1.65)	(1.02)	(0.63)

Concluding Remarks

The beam tests of the SCRFQ with a N^+ beam showed following results: 1) the transmission efficiency exceeds 90% at a design voltage, 2) the form of the transmission measured as a function of the intervane voltage and the emittance profiles of the output beam agree well with PARMTEQ prediction.

The beam tests of the SCRFQ/IH linac with a N^{2+} beam showed following results: 1) for five operating modes, the output beam energy and its spread agree fairly well with the design values, when the gap voltage and accelerating phase of each tank of the rebuncher and IH linac are set to the design values, and 2) the transmission efficiency of the IH linac is nearly 100%, when the transverse focusing elements are optimized. From the beam test results obtained so far, we can say the performance of the SCRFQ/IH linac is close to the designed one.

Acknowledgments

References

[1] T. Nomura, "Exotic Nuclei Arena in Japanese Hadron Project", INS-Report-780 (1989).

[2] S. Arai et al., "Construction and Beam Tests of a 25.5-MHz Split Coaxial RFQ for Radioactive Nuclei", INS-Rep.-1152 (1996).

[3] M. Tomizawa et al., "Model Measurement and Present Status of Interdigital-H Linac at INS", Proc. 1994 Int. Linac Conf., Tsukuba, 1994, p. 765.

[4] K. Niki et al., "Beam Transport Design for the Linac System in the INS Radioactive Beam Facility", ibid., p. 725.

[5] K. Yoshida et al., "Model Test of a Double-Coaxial $\lambda/4$ Resonant Cavity as a Rebuncher", ibid., p. 771.

[6] K. Crandall, "Effects of Vane-Tip Geometry on the Electric Fields in Radio-Frequency Quadrupole Linacs", LA9695-MS (1983).